Dispersion Analysis and Engineering in TiN 2D Plasmonic Waveguides

Conference Paper · February 2015

DOI: 10.1117/12.2076651

3 authors:

Hosam Mekawey
The American University in Cairo
9 PUBLICATIONS **32** CITATIONS
SEE PROFILE

Yehea Ismail
The American University in Cairo
454 PUBLICATIONS **4,242** CITATIONS
SEE PROFILE

Mohamed A Swillam
The American University in Cairo
263 PUBLICATIONS **1,618** CITATIONS
SEE PROFILE

Dispersion Analysis and Engineering in TiN 2D Plasmonic Waveguides

Hosam Mekawey[1]*, Yehea Ismail[1], and Mohamed A. Swillam[2]

[1]Center of Nanoelectronics and Devices (CND), The American University in Cairo, Zewail City of Science and Technology , Cairo, Egypt.

[2]School of Science and Engineering, The American University in Cairo, New Cairo, 11835

*hmekawey@aucegypt.edu

An investigation has been performed of the low order guided modes in TiN 2D hollow metallic waveguide. The dispersion characteristics of the TiN 2D hollow metallic waveguides key guided modes are identified and analyzed. Dispersion manipulating is proposed by changing the material of the cladding region. The dispersion analysis of 2D plasmonic waveguide using TiN has been investigated for the first time and compared to that of silver. A study has been conducted on the effect of varying the material on the cutoff in the modes dispersion. The effect of changing the plasmonic material on the dispersion curve key characteristics is also identified. Finally the effect of shifting the cutoff on the enhanced transmission phenomena is investigated.

1. INTRODUCTION

The possibility of increased confinement of the propagating modes is offered through plasmonic waveguides, promising a subwavelength photonic infrastructure suitable for integration on Silicon based photonic chips [1]. Plasmonic waveguides could help in reducing the size mismatch between electronic systems with footprint currently as small as 22 nm and typical photonic devices usually being built on the scale slightly smaller than the light wavelength at best [43]. Plasmonic waveguides suffer, however, from the drawback of increased losses, yet many applications, like sensing and extraordinary transmission [36-39], that lack the need of large propagation length, are not hindered by such drawback. Metallic gap [2-4], wedge [5], groove [6], nanowires [7], and the Metal-Insulator-Metal (MIM) plasmonic waveguide structures have been proposed. A great attention for MIM and IMI structures in particular are in the literature from many researchers due to the realitive simplicity of their manufacturing process and the range of interesting applications they possess [8-19], such as negative refractive index and slow light [20-24], sensing and interconnects applications [25] and in multiplexed sensing using Mach-Zehnder interferometer [26]. MIM and IMI plasmonic waveguides received a detailed study for their guided modes in the symmetric and asymmetric cases of the claddings [9]. The long-range propagation and high spatial confinement characteristics of the $Ag/SiO_2/Ag$ MIM waveguide guided modes have been studied numerically before [25]. In the work presented here, we investigate whether rectangular waveguide can offer MIM applications for both polarizations. Most of the studies for the rectangular plasmonic waveguide type focused on a certain effect or phenomenon at a specific wavelength band [27-28]. Rectangular plasmonic waveguide is expected to offer greater capabilities in comparison to MIM since rectangular metallic waveguide can offer the MIM capabilities for both polarization as found in [29] instead of single polarization as in MIM. Rectangular plasmonic waveguide offers sensing and energy transmission applications and shows much higher sensitivity than MIM waveguide [29]. Dispersion engineering of rectangular plasmatic waveguide using shape variation from rectangular to trapezoidal shape has been the focus of the work in [45]. The focus of the work presented here is on dispersion manipulation using Titanium Nitride (TiN) as a material variation compared to silver. TiN is selected for the study as a plasmonic material since it has recently received attention in literature as a possible alternative

Photonic and Phononic Properties of Engineered Nanostructures V, edited by Ali Adibi, Shawn-Yu Lin, Axel Scherer, Proc. of SPIE Vol. 9371, 93711C · © 2015 SPIE
CCC code: 0277-786X/15/$18 · doi: 10.1117/12.2076651

plasmonic material to noble metal plasmonic materials like gold and silver. TiN has been demonstrated to show plasmonic behavior in the visible and near-IR frequencies. TiN also demonstrates better performance in transformation optics and metamaterial devices than conventional gold and silver plasmonic materials. An inherit advantage of TiN is that it is compatible with standard silicon manufacturing processes, unlike gold and silver [34].

In the work presented here, we first briefly review in the second section the formulation for the MIM lowest order guided modes as well as the numerical analysis approach adopted in this work that is based on full vectorial finite element analysis and employed in the commercially available tool [30]. We then focus on identifying the key low order guided modes in TiN rectangular plasmonic waveguide with air filling. In section 3, The dispersion analysis of modes of interest in the 2D TiN plasmonic waveguide has been investigated for the first time in comparison to that of silver cladding. The effect of varying the cladding plasmonic material from silver to TiN on the dispersion of key guided modes is discussed. In section 4, an investigation of the effect of cutoff shift on enhanced transmission peaks is conducted. Finally, the conclusion is given in section 5.

2. RECTANGULAR PLASMONIC WAVEGUIDE KEY GUIDED MODES

MIM Waveguide Key Guided Modes Formulation

We expect that the guided modes in rectangular plasmonic waveguide will be related to or derived from the guided modes in MIM waveguides, as rectangular plasmonic waveguide with dielectric filling can be viewed as the intersection between a horizontal MIM waveguide and a vertical MIM waveguide. Hence, it is worth highlighting the MIM waveguide guided modes dispersion before embarking on performing numerical modal analysis for rectangular metallic. It has been shown from the MIM waveguide analysis of lowest order modes in [9]and [31] that when the upper and lower claddings are made from the same metal, the dispersion relation can be split into a pair of equations: one equation represents odd modes where Ez is odd while Hx and Ey are even for the coordinate system shown in Fig 1 while the other equation represents even mode (Ez is even while Hx and Ey are odd) Hence, for MIM waveguide structure, it is expected to find a fundamental even mode as well as a fundamental odd mode.

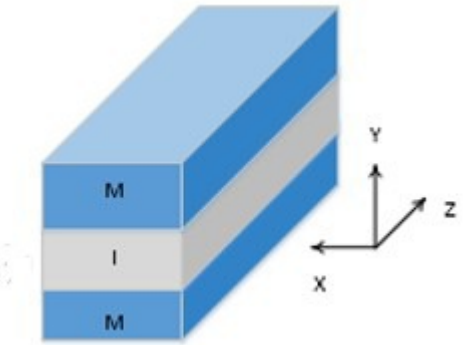

Fig 1: Geometry of an MIM waveguide where the direction of propagation is in the z direction.

Numerical Method and Geometrical Structure

Numerical modal analysis of 2D rectangular plasmonic waveguide by solving a full vectorial wave equation using the finite element method is the analysis approach selected in the work presented here. Full vectorial wave equation solution using finite element takes into account polarization coupling and allows for high index differences in the waveguide being simulated. Fig 2 shows the rectangular plasmonic waveguide geometrical structure. The dielectric filling to have a width of 270 nm and a height of 105 nm which is a typical size that has

been used throughout the paper as well as in other literatures for studying the enhanced transmission phenomena in rectangular holes [28][32]. Periodic boundary conditions are employed to facilitate a study of the extraordinary transmission (EOT) phenomena [37][38] later in this paper. The distance from dielectric center to adjacent dielectric center in a hole array is 450 nm in the x direction and 300 nm in the y direction.

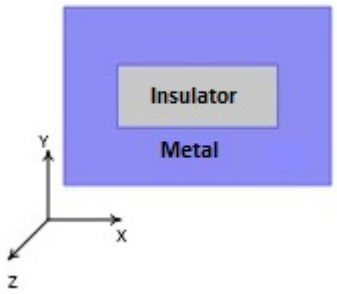

Fig 2: Geometric structure for rectangular plasmonic waveguide. The region labeled (Metal) is the metallic region while the area labeled (Insulator) is the dielectric region. The dimension for the dielectric region is 270x105 nm.

TiN Rectangular Plasmonic Waveguide Key Guided Modes

An Investigation has been conducted for the key guided modes in TiN rectangular plasmonic waveguide with the geometry shown in Fig 2 and dimension 270x105 nm where the cladding region is chosen to be TiN while the dielectric is air. Naik's experimental values for the TiN material dielectric function are used [35]. Four low order key guided modes have been identified and shown in Fig 3 as a result of the numerical modal analysis using Comsol [30]. There is a resemblance between the four guided modes and the odd and even modes components parity of the vertical and horizontal boundaries of the dielectric rectangular region if both of them act as MIM waveguides. The Vertical Odd (VO) mode profile in Fig 3.a, 3.b, and 3.c below has a low order odd Ez component and a low order even Ex and Hy components which resembles the profile of the odd mode in a vertical MIM waveguide (parallel to Y- axis) [9] [31]. In addition, the Vertical Even (VE) in Fig 3.d, 3.e, and 3.f matches the expected profile for a vertical MIM even mode as it has even Ez and odd Ex and Hy components. In a similar manner, the mode profiles for HO and HE shown from Fig 3.g, to Fig 3.l resemble the key odd and even modes of horizontal MIM waveguide (parallel to x axis) [9] [31]. This indicates that the rectangular plasmonic waveguide key guided modes might be related to or derived from the key guided modes of the two MIM waveguides formed from the vertical and horizontal boundaries of the rectangular waveguide. As a result, some of the benefits of the guided modes of two MIM waveguides of different sizes could be encapsulated in the guided modes of a single rectangular waveguide with TiN cladding. In order to investigate that, dispersion analysis is needed.

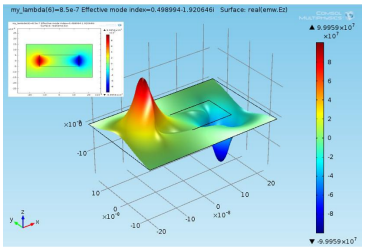

(a) VO: Ez

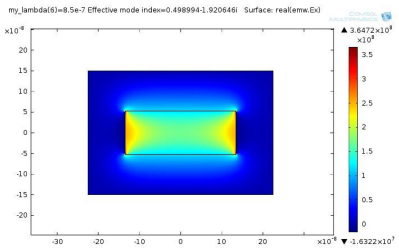

(b) VO: Ex

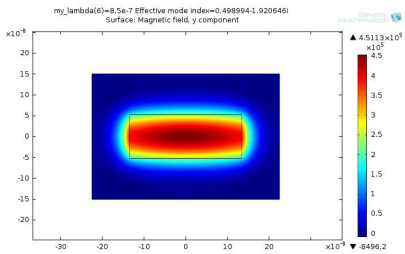

(c) VO: Hy

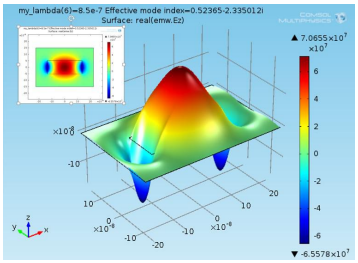

(d) VE: Ez

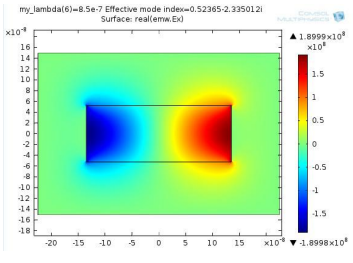

(e) VE: Ex

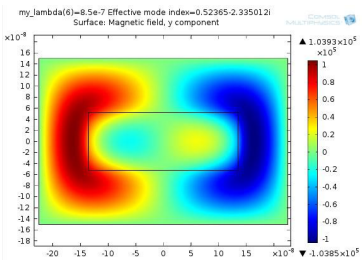

(f) VE: Hy

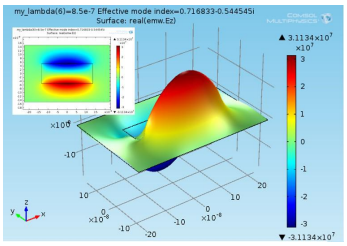

(g) HO: Ez

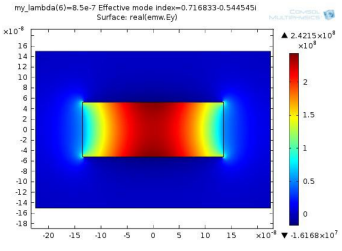

(h) HO: Ey

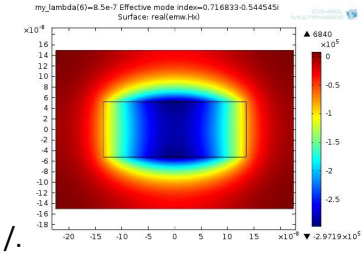

/.

(i) HO: Hx

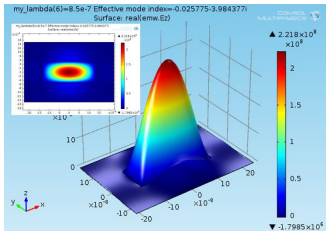

(j) HE: Ez

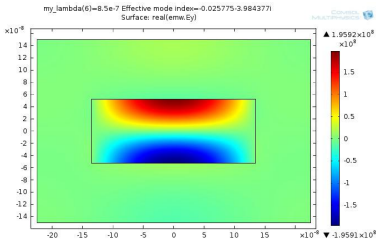

(k) HE: Ey

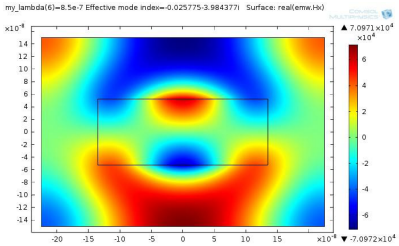

(l) HE: Hx

Fig 3: Mode profiles for the lowest order modes (named VO, VE, HO, and HE) in rectangular metallic waveguide. The dielectric filling is air while the metal is TiN. The dimensions of the waveguide dielectric filling is 270x105 nm. Sub figures from (a) to (l) show the respective modes profiles written in their captions. (a), (b) and (c) show that Ez is odd while Ex and Hy are even in the lowest order odd mode VO. (d), (e) and (f) show that Ez is even while Ex and Hy are odd in the lowest order even mode (VE). (g), (h) and (i) show that Ez is odd while Ey and Hx are even in the lowest order odd mode (HO). (j), (k), and (l) show that Ez is even while Ey and Hx are odd in the lowest order even mode (HE). The insets in (a), (d), (g), and (j) represent the xy projection of their respective mode profiles. The generated mode profiles are at wavelength 850 nm.

3. DISPERSION ANALYSIS: SILVER VERSUS TITANIUM NITRIDE CLADDING

In order to investigate the TiN material effect compared to traditional noble metal plasmonic material, a comparison of the dispersion relation for the four key guided modes VO, VE, HO, and HE when using silver versus TiN as cladding are shown in Fig 4. Palik's experimental values for the permittivity of silver have been utilized [33]. The horizontal axis represents the wavelength while the vertical axis represents the effective index. It is noticed that a rectangular waveguide of size 270x105 nm offers a cutoff in the VO and VE guided modes at around 440 nm and another cutoff in the HO and HE guided modes at 760 nm and 330 nm respectively in the silver cladding case. The cutoff for the TiN dispersion curve of the VO mode is around 600 nm wavelength at an effective index around 0.5 while for the HO mode, the cutoff is around 1100 nm. The peak in the HO mode of the TiN case is at 600 nm and is lower than that of the silver HO mode peak. Fig 4-(a), (b), and (c) indicate that both VO, HO and HE dispersion peak and cutoff suffer from red shift in the case of TiN when compared to silver. Also for VO, HO, and VE as shown in (a), (b) and (d) the cutoff in case of TiN happens at an effective index around 0.5 instead of 0 as in the case of silver waveguide. In (d), the dispersion peak for TiN VE mode is very small and slightly red shifted compared to silver. The peak height in the TiN VO mode is almost half of that of the silver VO mode. The dispersion of the

guided modes VO and VE for the vertical (short) boundaries are very similar regardless of the material. In general, when comparing HO dispersion curve and VO curve we notice that the general shape of the curve is similar, yet HO guided mode has its cutoff red shifted compared to the cutoff in VO curve. This can be a possible indication that when increasing the length of certain boundaries in the dielectric region boundaries, a red shift happens in the cutoff of their respective odd mode since the length of the horizontal boundaries causing HO is larger than that of the vertical boundaries causing VO. It is noticed also that VO and HO curves have their dispersion peak at approximately the same wavelength in the silver case. This indicates that although increasing the length of any of the dielectric region boundaries (vertical or horizontal) causes red shift in the cutoff of its respective odd mode (VO or HO), this does not red shift the dispersion peak as well when the cladding material is silver. By red shifting the cutoff while the peak still at the same position, a stretch of the region from the peak to the cutoff occurs. Hence, the slope of such region can be manipulated by adjusting the length of the dielectric region boundaries when using silver. In the TiN case, the peak is extended and becomes broader instead of being shifted. Although the dispersion curves for VO and VE caused by the vertical (short boundaries) are almost identical, this is not the case for the dispersion curves of HO and HE caused by the horizontal (long) boundaries. The HE guided mode of the rectangular waveguide has a negative effective index at certain intervals. This can be explained that the wave in the HE mode is a backward wave [24] at such wavelength intervals. It is worth noting that the HO and VO guided modes are similar, in terms of spatial mode profile, to the widely known TE_{10} and TM_{11} guided mode profiles respectively in rectangular metallic waveguide at microwave frequencies. However, there is a red shift in the cutoff wavelength of the HO mode compared to the TE_{10} microwave guided mode. As indicated in Fig 4, the cutoff wavelength of the HO mode is around 760 nm for silver and 1100 nm for TiN while the cutoff wavelength for a TE_{10} microwave mode in a rectangular waveguide of 270x105 nm should be around 2*270=540 nm [44]. A detailed study of the red shift in the cutoff of TE_{10} mode due to plasmonic effect is published earlier [42]. Also for the TM_{11} microwave mode, it is expected that the cutoff wavelength for a 270x105 nm rectangular waveguide to be around 195 nm [44], however the cutoff wavelength of the VO guided mode is around 440 nm in silver and 600 nm in TiN, as shown in Fig 4-a, indicating a red shift as well.

What has been shown in this section represents an example on shifting the dispersion curve key characteristics using material manipulation. By selecting the appropriate plasmonic material, the waveguide designer can tune the rectangular waveguide to exploit its applications at different frequency ranges.

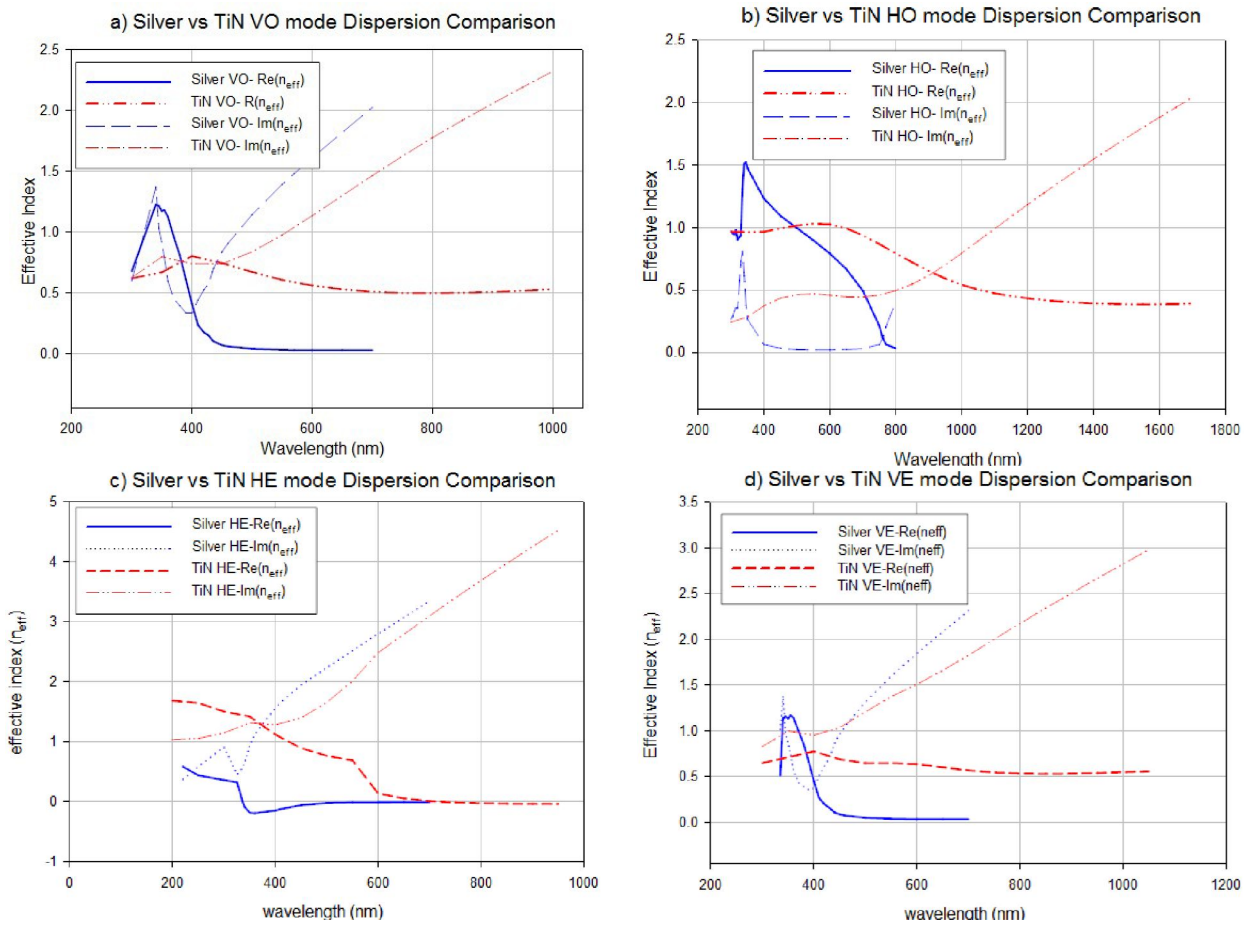

Fig 4: Comparison between the dispersion relation of VO, HO, HE, and VE modes in silver versus TiN cladding. The waveguide in both cases is a rectangular waveguide 270x105 nm with air hole. (a), (b), and (c) indicates that both VO, HO and HE dispersion peak and cutoff suffers from red shift in the case of TiN when compared to Silver. Also for VO, HO, and VE as shown in (a), (b) and (d) the cutoff in case of TiN happens at an effective index around 0.5 instead of 0 as in the case of silver waveguide. In (d), the dispersion peak for TiN VE mode is very small and slightly red shifted compared to silver.

4. NEAR CUTOFF ENHANCED TRANSMISSION ANALYSIS IN SILVER AND TITANUM NITRIDE

In this section an analysis of the near cutoff enhanced transmission [27-28] [32] [36-39] in rectangular TiN and silver waveguides is presented. The objective is to investigate the effect of the red shift that has been reported in the TiN HO mode cutoff on the enhanced transmission phenomena for the rectangular structure. The objective as well is to investigate the effect of having a dispersion cutoff at 0.5 effective index in TiN HO mode instead of near zero effective index on the near cutoff enhancement. Numerical simulation using FDTD photonic simulation package [40] has been used as the chosen approach for the enhanced transmission analysis. The simulated structure consists of a plasmonic material (TiN/silver) wall (modeled using Lorentz-Drude model) that has an air hole at its center with dimensions 270x105. The thickness of the material wall is 300 nm. Periodic boundaries are utilized in the transverse plan while anisotropic PML boundaries are utilized as the z plan boundaries. The source is a y-polarized Gaussian modulated continuous wave with wavelength 700 nm. Fig 9 shows the power spectrum normalized to the input power and the area for the rectangular air hole with silver cladding (solid line) and TiN cladding (dashed line). From Fig 5, the enhanced transmission peak in TiN is red shifted in correspondence to the cutoff red shift that has been reported in the previous section for the TiN rectangular waveguide HO mode in comparison to the silver HO mode. However, the red shift is a slight shift also the enhancement is much weaker

enhancement than silver. This is probably due to the cutoff of the TiN HO mode being near 0.5 effective index instead of zero as in silver. The enhanced transmission curve of the silver shows as well the well-known Rayleigh minima of Wood's anomaly [41] reported before in similar enhanced transmission calculation by Ebbesen [37].

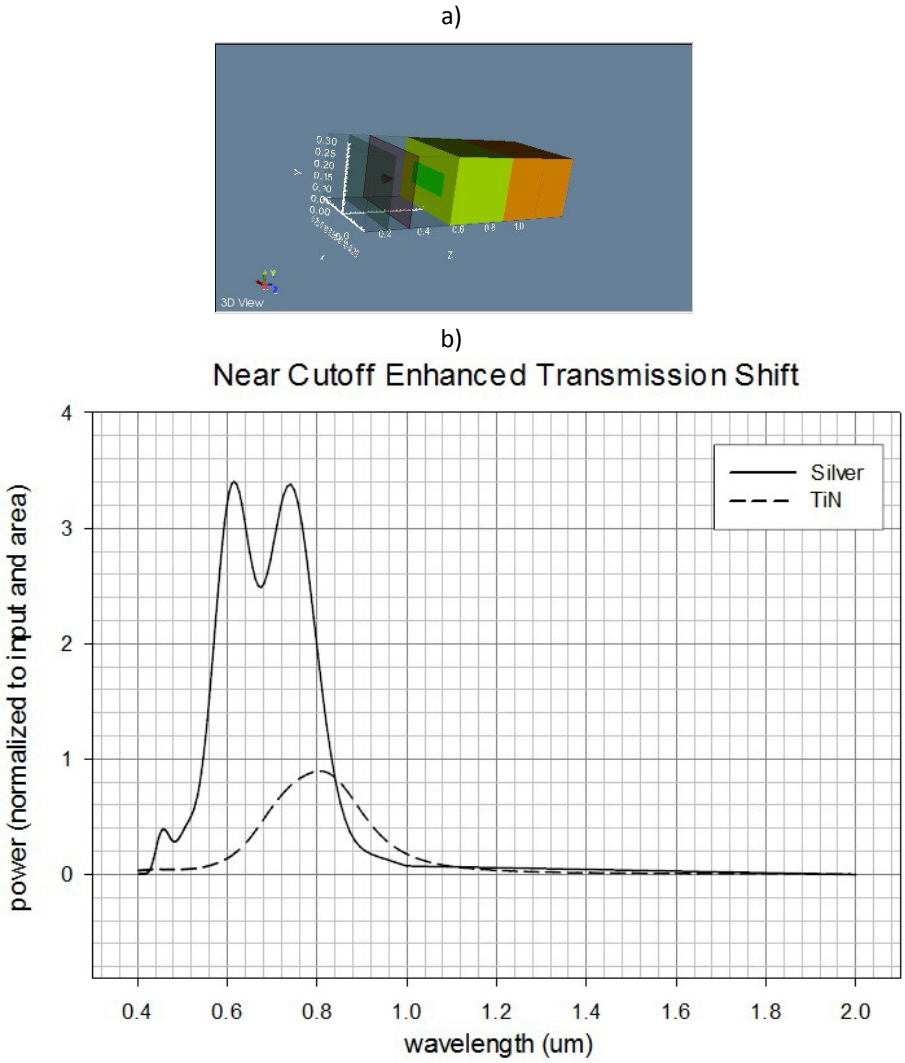

Fig 5: The enhanced transmission phenomena observed in a simulation for a TiN (dashed) and silver (solid) wall with air hole. The vertical axis in (b) represents the transmitted power normalized to the input power and area. The curves indicate a slight red shift in the enhanced transmission peak of the TiN material that corresponds to the red shift in its HO mode cutoff compared to silver cutoff yet with significant reduction in enhancement. The minima shown in the silver enhancement curve correspond to the Rayleigh minima of Wood's anomaly [41]. (a) shows 3D schematics of the structures being simulated using Optiwave FDTD package [40].

5. CONCLUSION

In this paper a modal analysis of the key low order guided modes in 2D rectangular plasmonic waveguide has been conducted which reveals the existence of four low order guided modes: VO odd mode, VE even odd, HO odd mode and HE even mode. The VO odd mode and VE even mode are related to an MIM waveguide modes formed by the

dielectric region vertical boundaries. Similarly the HO and HE modes are related to an MIM waveguide modes formed by the horizontal boundaries. Dispersion analysis of the 4 guided modes of the rectangular plasmonic waveguide, with silver and TiN cladding, shows that each of the HO mode and the VO mode dispersion has a cutoff wavelength. The cutoff of the HO mode happens at a wavelength larger than that of the cutoff wavelength of the VO mode due to longer horizontal boundaries in comparison to the vertical boundaries of the dielectric region in the rectangular waveguide studied in this work. This implies that the cutoff location can be controlled by controlling the boundaries lengths. It implies as well that by using rectangular plasmonic waveguide we would gain the benefits of 2 wavelength cutoffs at different wavelengths proportional to the dielectric boundaries length. A cutoff in the dispersion can be exploited in applications like filtering and near cutoff extraordinary transmission phenomena [38]. Such phenomena provides an interesting capability of transporting the electromagnetic energy with minimum losses by tunneling [36-39]. Altering the cladding material to shift the cutoff in order to exploit its related applications in a desired wavelength range is investigated. By using TiN instead of silver as a plasmonic material for the cladding, a red shift was identified in the dispersion cutoff and peak for the VO and HO modes in TiN rectangular waveguide compared to their counterparts when using silver. This demonstrates an approach for shifting and engineering the dispersion by varying the dielectric material rather than the shape or the dimension of the waveguide. Finally we investigated the near cutoff extraordinary transmission phenomena [36-39] in the TiN rectangular waveguide in comparison to the silver and the extraordinary transmission peak is found to slightly red shifted in the case of TiN in correspondence to the red shift in the TiN HO mode cutoff. The enhancement however in TiN is much weaker than in silver and the red shift is small probably due to the cutoff of the TiN HO mode being near 0.5 effective index instead of zero as in silver.

6. ACKNOWLEDGEMENT

This research was partially funded by Zewail City of Science and Technology, American University in Cairo (AUC), SemiConductor Research Cooperation, Global Foundries, the STDF, Intel, Mentor Graphics, and MCIT.

REFERENCES

[1] Maier, S. A., "Plasmonics: The Promise of Highly Integrated Optical Devices," *IEEE Journal of Selected Topics in Quantum Electronics,* vol. 12, no. 6, pp. 1671-1677, (2006).

[2] Tian, J., Yu, S., Yan, W., Qiu, M., "Broadband high-efficiency surface-Plasmon-polariton coupler with silicon-metal interface," *Applied Physics Letters,* vol. 95, no. 1, (2009).

[3] Wang, B., Wang, G. P., " Surface plasmon polariton propagation in nanoscale metal gap waveguides," *Opt. Lett.,* vol. 29, no. 17, p. 1992–1994, (2004).

[4] Maier, S. A., "Gain-assisted propagation of electromagnetic energy in subwavelength surface plasmon polariton gap waveguides," *Opt. Commun.,* vol. 258, p. 295–299, (2006).

[5] Moreno, E., Rodrigo, S. G., Bozhevolnyi, S. I., Martín-Moreno, L. , García-Vidal, F. J.,"Guiding and focusing of electromagnetic fields with wedge plasmon polaritons," *Phys Rev Lett,* vol. 100, (2008).

[6] Bozhevolnyi, S. I., Volkov, V. S., Devaux, E., Laluet , J.-Y., Ebbesen, T. W., "Channel plasmon subwavelength waveguide components including interferometers and ring resonators," *Nature,* vol. 440, pp. 508-511, (2006).

[7] Fang, Y., Li, Z., Huang, Y., Zhang, S., Nordlander, P., Halas, N. J., Xu, H., "Branched Silver Nanowires as Controllable Plasmon Routers," *Nano Lett.,* vol. 10, no. 5, p. 1950–1954, (2010).

[8] Economou, E., "Surface Plasmons in Thin Films," *Phys. Rev.,* vol. 182, pp. 539-554, (1969).

[9] Prade, B., Vinet, J. Y. , Mysyrowicz, A., "Guided optical waves in planar heterostructures with negative dielectric constant," *Phys. Rev B,* vol. 44, no. 24, pp. 13556--13572, (1991).

[10] Hu, H., Zeng, X., Tong, C., Anderson, W. A., Gan, Q., Deng, J., Jiang, S., "Polarization-Insensitive Metal–Semiconductor–Metal Nanoplasmonic Structures for Ultrafast Ultraviolet Detectors," *J. Plasmonics,* vol. 8, no. 2, pp. 239-247, (2013).

[11] Berini, P., "Long-range surface plasmon polaritons," *Adv. Opt. Photon.,* vol. 1, pp. 484-588, (2009).

[12] Maier, S. A., "Plasmonics: Metal Nanostructures for Subwavelength Photonic Devices," *Selected Topics in Quantum Electronics, IEEE Journal of ,* vol. 12, no. 6, pp. 1214-1220, (2006).

[13] Burke, J. J. , Stegeman, G. I., "Surface-polariton-like waves guided by thin, lossy metal films," *Phys. Rev. B,* vol. 33, no. 8, p. 5186–5201, (1986).

[14] Pannipitiya, A., Rukhlenko, I., Premaratne, M., Hattori, H., Agrawal, G., "Improved transmission model for metal-dielectricmetal plasmonic waveguides with stub structure," *Opt. Express,* vol. 18, pp. 6191-6204, (2010).

[15] Park, J., Kim, K., Lee, I., Na, H., Lee, S., Lee, B., "Trapping light in plasmonic waveguides," *Opt. Express,* vol. 18, pp. 598-623, (2010).

[16] Lin, C.-I., Gaylord, T. K., "Multimode metal-insulator-metal waveguides: Analysis and experimental characterization," *Phys. Rev. B,* vol. 85, p. 085405, (2012).

[17] Zia, R., Selker, M., Catrysse, P., Brongersma, M., "Geometries and materials for subwavelength surface plasmon modes," *J. Opt. Soc. Am. A,* vol. 21, pp. 2442-2446, (2004).

[18] Kocabaş, Ş. E., Veronis, G., Miller, D. A. B. , Fan, S., "Modal analysis and coupling in metal-insulator-metal waveguides," *Phys. Rev. B,* vol. 79, p. 035120, (2009).

[19] Kong, X., Li, Z., Tian, J., "Mode converter in metal-insulator-metal plasmonic waveguide designed by transformation optics," *Opt. Express,* vol. 21, pp. 9437-9446, (2013).

[20] Lezec, H. J., Dionne, J. A., Atwater, H. A., "Negative refraction at visible frequencies," *Science,* vol. 316, no. 5823, p. 430–432, (2007).

[21] Yang, T., K. Crozier, "Analysis of surface plasmon waves in metaldielectric- metal structures and the criterion for negative refractive index," *Opt. Express,* vol. 17, pp. 1136-1143, (2009).

[22] Dionne, J. A., Verhagen, E., Polman, A., Atwater, H. A., "Are negative index materials achievable with surface plasmon waveguides ? A case study of three plasmonic geometries," *Opt. Express,* vol. 16, no. 23, p. 19001–19017, (2008).

[23] Alu, A., Engheta, N., "Optical nanotransmission lines: synthesis of planar left-handed metamaterials in the infrared and visible regimes," *J. Opt. Soc. Am. B,* vol. 23, no. 3, p. 571–583, (2006).

[24] Davoyan, A., Bozhevolnyi, S., Kivshar, Y., Shadrivov, I., "Backward and forward modes guided by metal-dielectric-metal plasmonic waveguides," *J. Nanophoton.,* vol. 4, no. 1, pp. 043509-043509, (2010).

[25] Dionne, J. A., Sweatlock, L. A., Atwater, H. A., Polman, A., "Plasmon slot waveguides: Towards chip-scale propagation with subwavelength-scale localization," *Phys. Rev. B,* vol. 73, no. 3, p. 035407, (2006).

[26] Zeng, X., Gao, Y., Hu, H., Ji, D., Gan, Q., Bartoli, F., "A metal-insulator-metal plasmonic Mach-Zehnder interferometer array for multiplexed sensing," *Journal of Applied Physics,* vol. 113, p. 133102, (2013).

[27] Garcia-Vidal, F. J., Martin-Moreno, L., Ebbesen, T. W., Kuipers, L., "Light passing through subwavelength apertures," *Rev. Mod. Phys.,* vol. 82, no. 1, pp. 729-787, (2010).

[28] Garcı´a-Vidal, F. J., Moreno, E., Porto, J. A., Martin-Moreno, L., "Transmission of Light through a Single Rectangular Hole," *Phys. Rev. Lett.,* vol. 95, no. 10, p. 103901, (2005).

[29] Swillam, M. A., Helmy, A. S., "Analysis and applications of 3D rectangular metallic waveguides," *Optics Express,* vol. 18, no. 19, pp. 19831-19843, (2010).

[30] www.comsol.com, "Comsol Multiphysics: RF Module User Guide," COMSOL, Inc, Stockholm, (2013).

[31] Maier, S. A., [Plasmonics: Fundamentals and Applications], Springer, (2007).

[32] García-Vidal, F. J., Martín-Moreno, L., Moreno, E., Kumar, L. K. S., Gordon, R., "Transmission of light through a single rectangular hole in a real metal," *Phys. Rev. B,* vol. 74, p. 153411, (2006).

[33] Palik, E. D., [Handbook of optical constants of solids], Academic Press, Inc., (1985).

[34] Naik, G. V., Schroeder, J. L., Ni, X., Kildishev, A. V., Sands, T. D., Boltasseva, A., "Titanium nitride as a plasmonic material for visible and near-infrared wavelengths," *Opt. Mater. Express,* vol. 2, no. 4, pp. 478-489, (2012).

[35] Naik, G. V., Kim, J., Boltasseva, A., "Oxides and nitrides as alternative plasmonic materials in the optical range," *Opt. Mater. Express,* vol. 1, no. 6, pp. 1090-1099, (2011).

[36] Degiron, A., Lezec, H., Yamamoto, N., Ebbesen, T., "Optical transmission properties of a single subwavelength aperture in a real metal," *Optics Communications,* vol. 239, no. 1–3, pp. 61-66, (2004).

[37] Martín-Moreno, L., García-Vidal, F. J., Lezec, H. J., Pellerin, K. M., Thio, T., Pendry, J. B., Ebbesen, T. W., "Theory of Extraordinary Optical Transmission through Subwavelength Hole Arrays," *Phys. Rev. Lett.,* vol. 86, no. 6, pp. 1114--1117, (2001).

[38] Ebbesen, T. W., Lezec, H. J., Ghaemi, H. F., Thio, T., "Extraordinary optical transmission through sub-wavelength hole arrays," *Nature,* vol. 391, pp. 667-669, (1998).

[39] Weiner, J., "The physics of light transmission through subwavelength apertures and aperture arrays," *Rep. Prog. Phys.,* vol. 72, no. 6, p. 064401, (2009).

[40] Optiwave Systems, "OptiFDTD user Guide," Optiwave Systems Inc., Ottawa, (2013).

[41] Lord Rayleigh, "III. Note on the remarkable case of diffraction spectra described by Prof. Wood," *Philosophical Magazine Series 6,* vol. 14, no. 79, pp. 60-65, (1907).

[42] Gordon, R., Brolo, A., “Increased cut-off wavelength for a subwavelength hole in a real metal,” Opt. Express 13(6), 1933–1938, (2005).

[43] Lim, S., Png, C., Ong, E., Ang, Y., "Single mode, polarization-independent submicron silicon waveguides based on geometrical adjustments," Opt. Express 15, 11061-11072, (2007).

[44] Pozar, D. M., [Microwave Engineering], Wiley, (2012).

[45] Mekawey, H., Ismail, Y., Swillam, M., "Dispersion analysis and engineering of 2D plasmonic waveguides," J. Opt. 17, 015003 (2015).